Phase separation in Sr doped $BiMnO_3$*

Li Guan-Nan(李冠男)[a], Rao Guang-Hui(饶光辉)[b]†, Huang Qing-Zhen(黄清镇)[c], Gao Qing-Qing(高庆庆)[a], Luo Jun(骆 军)[a], Liu Guang-Yao(刘广耀)[a], Li Jing-Bo(李静波)[d], and Liang Jing-Kui(梁敬魁)[a]

[a] *Beijing National Laboratory for Condensed Matter Physics, Institute of Physics, Chinese Academy of Sciences, Beijing* 100190, *China*
[b] *School of Materials Science and Engineering, Guilin University of Electronic Technology, Guilin* 541004, *China*
[c] *NIST center for Neutron Research, National Institute of Standards and Technology, Gaithersburg, MD* 20899-8562, *USA*
[d] *School of Materials Science and Engineering, Beijing Institute of Technology, Beijing* 100081, *China*

(Received 12 September 2013; revised manuscript received 9 October 2013; published online 24 January 2014)

Phase separation in Sr doped $BiMnO_3$ ($Bi_{1-x}Sr_xMnO_3$, $x = 0.4$–0.6) was studied by means of temperature-dependent high-resolution neutron powder diffraction (NPD), high resolution X-ray powder diffraction (XRD), and physical property measurements. All the experiments indicate that a phase separation occurs at the temperature coinciding with the reported charge ordering temperature (T_{CO}) in the literature. Below the reported T_{CO}, both the phases resulting from the phase separation crystallize in the orthorhombically distorted perovskite structure with space group *Imma*. At lower temperature, these two phases order in the CE-type antiferromagnetic structure and the A-type antiferromagnetic structure, respectively. However, a scrutiny of the high-resolution NPD and XRD data at different temperatures and the electron diffraction experiment at 300 K did not manifest any evidence of a long-range charge ordering (CO) in our investigated samples, suggesting that the anomalies of physical properties such as magnetization, electric transport, and lattice parameters at the T_{CO} might be caused by the phase separation rather than by a CO transition.

Keywords: phase separation, neutron/X-ray powder diffraction, charge/orbital order

PACS: 64.75.Qr, 75.25.Dk, 71.30.+h **DOI:** 10.1088/1674-1056/23/3/036401

1. Introduction

Perovskite manganites have been extensively studied due to their fascinating phenomena in structure, magnetic and electronic transitions. The intriguing phenomena are derived from the interplay among spin, charge, orbital and lattice degrees of freedom of the transition metal manganese.[1,2] In the conventional perovskite manganites with chemical formula $R_{1-x}M_xMnO_3$ (R = trivalent cation, M = divalent caiton), the charge order always accompanied by or followed an orbital order resulting from the cooperative Jahn–Teller distortion.[3,4] Among all the $R_{1-x}M_xMnO_3$, the charge ordering temperatures (T_{CO}) are below 300 K except for the Bi-based perovskite manganites $Bi_{1-x}M_xMnO_3$ (M = Ca, Sr). For $Bi_{0.5}Ca_{0.5}MnO_3$ and $Bi_{0.5}Sr_{0.5}MnO_3$, the T_{CO} were reported to be 325 K and 475 K, respectively.[5,6] In particular, a T_{CO} as high as 600 K was reported for the $Bi_{0.75}Sr_{0.25}MnO_3$.[7] It was argued that the $Bi^{3+}6s^2$ lone pair played a crucial role for stabilizing the CO state in the Bi-based perovskite manganites,[6] since a partial hybridization of the $Bi^{3+}6s^2$ lone pair with O 2p orbitals reduced the mobility of the e_g electrons through Mn–O–Mn bonds and enhanced the electronic localization. However, a new kind of charge ordering type discovered by Hervieu *et al* and the absence of Bi/Sr ordering in $Bi_{1-x}Sr_xMnO_3$ pose a question on the role of the Bi^{3+} lone pair for stabilizing the CO state.[8] A recent study on $Bi_{0.6}Ca_{0.4}MnO_3$ single crystals proposed a high stability of the CO/OO state with an ordered double band of MnO_6 and suggested an absence of real space Mn^{3+}/Mn^{4+} ordering of the ionic picture.[9,10] In most publications, the CO state is characterized by the anomalies in resistivity, magnetization, and lattice distortion at T_{CO}.[11,12] Albeit all these features were observed, the compounds $Sm_{0.15}Ca_{0.85}MnO_3$ and $Ca_{1-x}Bi_xMnO_3$ ($x \leq 0.25$) showed no evidence of long-range charge ordering.[13,14] Instead, a phase separation behavior was observed in these compounds below the temperature where the anomalies took place. Coexistence of two phases down to 1.5 K has also been reported in $Bi_{0.5}Sr_{0.5}MnO_3$ which was supposed to have an extremely high T_{CO}.[15] Interestingly, these two phases have almost the same chemical composition and both crystallize in the orthorhombically distorted perovskite structure with space group *Pnma*. The authors claimed that the charge order state existed exclusively in the majority phase while the minority phase showed no charge order, implying the CO/OO state is sensitive to a tiny composition fluctuation in this compound. The extremely high T_{CO} in Bi-based perovskite manganites has triggered extensive interest of researchers, yet the mechanism remains unclear.

In this work, the structural evolution of the $Bi_{1-x}Sr_xMnO_3$ ($x = 0.4$–0.6) was studied around the reported

*Project supported by the National Natural Science Foundation of China (Grant Nos. 11074295 and 50872148) and the Natural Science Foundation of Guangxi Province, China (Grant No. 2012GXNSFGA060002).

†Corresponding author. E-mail: ghrao@iphy.ac.cn; rgh@guet.edu.cn

© 2014 Chinese Physical Society and IOP Publishing Ltd

T_{CO} by temperature-dependent high-resolution X-ray diffraction and neutron powder diffraction. The resistivity, magnetization, and Seebeck coefficient were also measured. Occurrence of phase separation around the reported T_{CO} was observed by detailed structural analysis and evidenced by concomitant anomalies in electric transport, magnetic susceptibility, and lattice parameters.

2. Experimental

Polycrystalline samples of $Bi_{1-x}Sr_xMnO_3$ ($x = 0.4, 0.5, 0.6$) were synthesized by the solid state reaction with stoichiometric powders of Bi_2O_3 (99.99%), $SrCO_3$ (99.99%), and MnO_2 (99.99%).The powders were mixed, ground, and calcined at 900 °C for 24 h. After calcination, the mixtures were pressed into pellets and sintered again in air at 1100 °C, 1150 °C, and 1200 °C for 24 h, respectively, with the Sr concentration increasing. Then, the samples were reground, pressed into pellets and sintered at the same temperatures for another 24 h, and finally furnace-cooled to room temperature.

The purity of the samples was checked by X-ray powder diffraction (XRD) using a PANalytical X'pert PRO high–resolution diffractometer. High-resolution neutron powder diffraction (NPD) data were collected at NIST–NCNR on the BT-1 high-resolution diffractometer, using monochromatic neutrons of wavelength 1.5403 Å. XRD data were collected on a PANalytical X'pert PRO Alpha-1 X-ray diffractometer with Cu $K_{\alpha 1}$ radiation ($\lambda = 1.54056$ Å) at the same temperatures as for collecting the NPD data. The XRD data used for Rietveld refinement of the crystal structure were collected in the 2θ range from 10° to 140° with a step size of 0.017°. A physical property measurement system (PPMS) facility (quantum design) was used for the magnetization measurements in the temperature range of 300 K–600 K. Resistivity was measured using the conventional four-probe method. The high temperature thermoelectric properties were measured using a Linseis instrument (LSR-3).

3. Results and discussion

The crystal structure of the polycrystalline $Bi_{1-x}Sr_xMnO_3$ ($x = 0.4$–0.6) at 300 K was refined, using the XRD data and the space group *Imma*. Figure 1 shows a selected region of the one-phase model and two-phase model refinements of the sample $Bi_{0.5}Sr_{0.5}MnO_3$ at 300 K and 12 K. When the one-phase model was used for the structure refinement, the experimental data could not be fitted satisfactorily by the theoretical profile function (pseudo-Voigt) for some peaks. As shown in Figs. 1(a) and 1(c), an obvious shoulder of the (202) peak is not accounted for by the theoretical profile. Thus a two-phase model was proposed and used for the refinement. The difference curve at the bottom in Fig. 1(b) is nearly flat, and the goodness of fitting factor R_{WP} is 6.3%, much smaller than that of the one-phase model ($R_{WP} = 10.7\%$). The refinement reveals that the crystal structure of all three samples is composed of two orthorhombic phases and the space group is *Imma* with four formulas per unit cell for both the phases. In order to determine the occupancy of the O atom, a joint refinement of the crystal structure was performed using both the XRD data and the NPD data collected at 300 K and the two-phase model. The refinement gives the phase fractions of 76.11(2) wt% and 23.89(2) wt%, respectively, for the two phases in $Bi_{0.5}Sr_{0.5}MnO_3$. In the majority phase (MA), the refined occupancies are 0.514(3), 0.486(3), 0.988(7), and 1.019(5) for Bi, Sr, O1 in 4*e* position and O2 in 8*g* position, respectively. The occupancy of O2 for the MA phase is larger than 1.0, which means a full occupancy and we fixed it to 1.0 in the refinement. In the minority phase (MI), the refined occupancies are 0.520(3), 0.480(3), 0.978(9), and 0.980(9) for Bi, Sr, O1 in 4*e* position and O2 in 8*g* position, respectively. A full occupancy of Mn in 4*b* position was assumed and fixed to 1.0 for both the phases in the refinement. For the refinements of the crystal structure at different temperatures, the atomic occupancies in the two phases were fixed to those derived from the joint refinement of NPD and XRD data at room temperature.

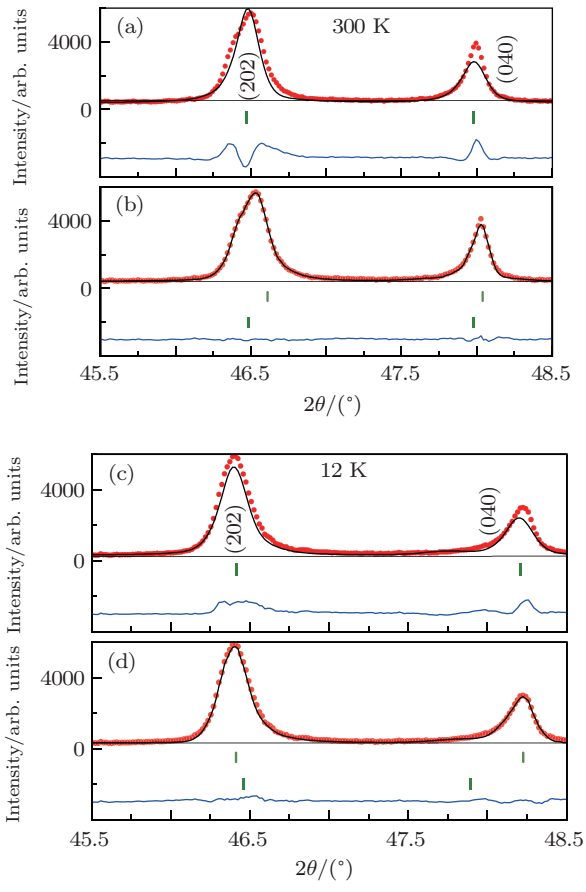


Fig. 1. (color online) Selected region of the Rietveld refinement plot of the XRD data for $Bi_{0.5}Sr_{0.5}MnO_3$ at 300 K and 12 K with one-phase model (panels (a) and (c)) and two-phase model (panels (b) and (d)).

At low temperature, detailed XRD and NPD experiments were performed. Figures 1(c) and 1(d) show a selected region of the refined XRD pattern of $Bi_{0.5}Sr_{0.5}MnO_3$ at 12 K. It is obvious that the two-phase model is more suitable than the one-phase model for the refinement. Figure 2 shows the portion of the NPD data of $Bi_{0.5}Sr_{0.5}MnO_3$ at 7 K ($< T_N$) and 200 K ($> T_N$). At low temperature, a series of additional Bragg peaks appeared in the low-angle range and were attributed to the magnetic contribution. All the magnetic reflections were indexed and could be assigned to either the A-type or the CE-type AFM structure.[16] The refinement of the NPD data at 7 K was done with the two-phase model and the refinement revealed that the magnetic space groups of the magnetic structures are $P2'/m$ and $I'm'm'a$ for the CE-type and the A-type magnetic structures, respectively. The CE-type structure belongs to the MI phase and the A-type structure belongs to the MA phase. The $P2'/m$ magnetic structure can only be indexed using the double lattice parameters a and c of the MI phase and the $I'm'm'a$ structure can be indexed using the unit cell parameters of the MA phase.

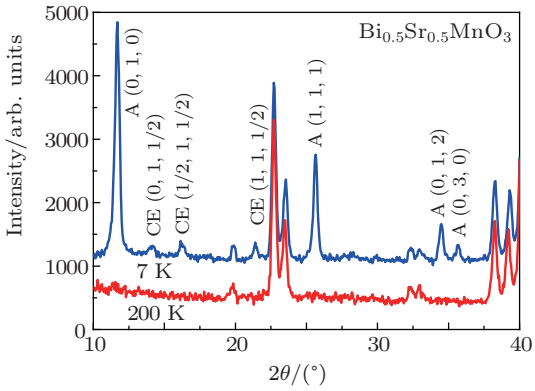


Fig. 2. (color online) Portion of the NPD patterns of $Bi_{0.5}Sr_{0.5}MnO_3$ collected at 7 K and 200 K. A group of magnetic peaks appear at 7 K and can be indexed by nuclear unit cell and $2a \times b \times 2c$ cell, respectively.

The temperature-dependent magnetization (M–T) of the $Bi_{1-x}Sr_xMnO_3$ ($x = 0.4$–0.6) was measured under a magnetic field of $H = 200$ Oe on cooling after a zero-field cooling (ZFC), as shown in Fig. 3. The magnetization curves exhibit a slope change at about 446 K, 485 K, and 450 K for $x = 0.4$, 0.5, and 0.6, respectively. Previous studies usually attributed this slope change to the charge ordering transition.[17] In this study, the temperatures corresponding to the slope change of the M–T curves are very close to the reported T_{CO}.[18]

High-flux BT9 triple-axis spectrometers were used to monitor the evolution of the magnetic peak intensity as a function of temperature below room temperature. The CE-type (1/2, 1/2, 0) peak and the A-type (0, 0, 1) peak of the $x = 0.5$ were chosen to be monitored as shown in the inset of Fig. 3. Upon heating, the long range magnetic order disappears at $\sim$ 160 K for both the phases in $Bi_{0.5}Sr_{0.5}MnO_3$. This temperature agrees with the reported antiferromagnetic transition temperature of the compound.[19]

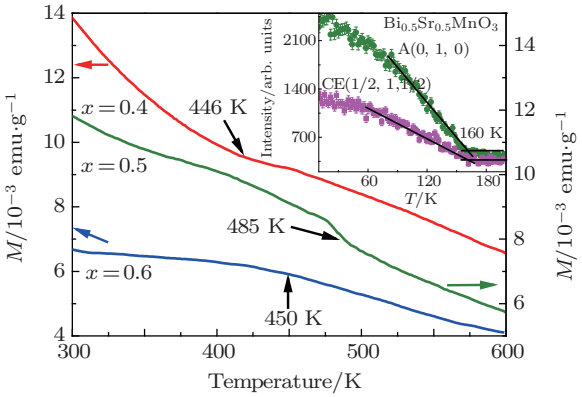


Fig. 3. (color online) Temperature dependence of the magnetization of $Bi_{1-x}Sr_xMnO_3$ at $H = 200$ Oe on cooling. The inset shows the temperature dependence of the peak intensities of the magnetic peaks of the CE-type and the A-type structures in NPD data for $Bi_{0.5}Sr_{0.5}MnO_3$ on warming, recorded by the high-flux BT-9 triple-axis spectrometer at NCNR.

The resistivity data of $Bi_{1-x}Sr_xMnO_3$ for $x = 0.4$, 0.5, and 0.6 are shown in Fig. 4(a), registered in the absence of an external applied magnetic field. The resistivity increases rapidly as the temperature decreases. There is a slope change of resistivity in logarithmic scale at 455 K, 495 K, and 465 K for $x = 0.4$, 0.5, and 0.6, respectively. The slope change is more prominent on the temperature dependence of thermoelectric power (S) of $Bi_{1-x}Sr_xMnO_3$, as shown in Fig. 4(b). For each investigated compound, the temperatures, at which the M–T (Fig. 3), R–T and S–T curves exhibit slope change, are close to each other and also close to the reported T_{CO} of the compounds.

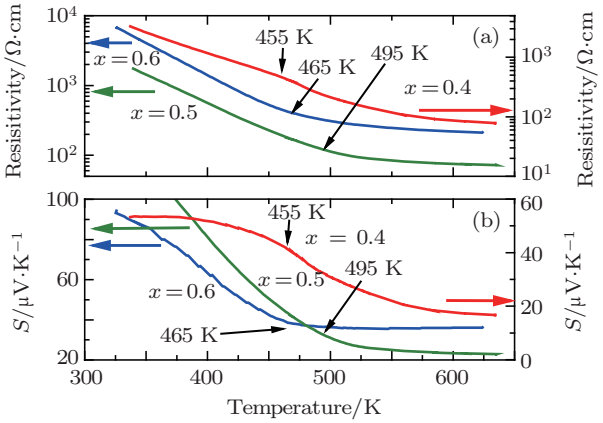


Fig. 4. (color online) Temperature dependence of resistivity (a) and thermoelectric power (b) of $Bi_{1-x}Sr_xMnO_3$ ($x = 0.4$, 0.5, and 0.6).

Above the reported T_{CO}, high resolution XRD experiments were performed for the sample $Bi_{0.5}Sr_{0.5}MnO_3$. Figure 5 shows the refinement result of the high-resolution XRD pattern at 570 K, which manifests that there is only one phase with the space group *Imma* in $Bi_{0.5}Sr_{0.5}MnO_3$ above the reported T_{CO}. The inset in Fig. 5 shows the enlarged view of

the refinement result for the (202) and (040) peaks. Compared with the results shown in Figs. 1(a) and 1(c), the difference curve indicates an excellent fitting between the theoretical and experimental data with the one-phase model at 570 K. The reliable factors of the refinement are $R_{WP} = 5.62\%$ and $\chi^2 = 1.83$, respectively. The refinement results of the XRD data at different temperatures suggest that the samples undergo a phase separation from one phase to two phases as the temperature decreases.

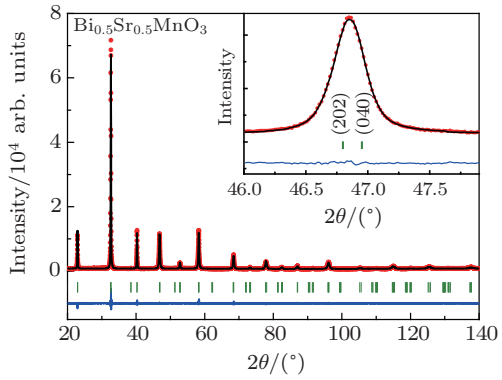


Fig. 5. (color online) Plot of observed and calculated XRD patterns for $Bi_{0.5}Sr_{0.5}MnO_3$ at 570 K. The short bars indicate the positions of Bragg reflections. The difference plot, I (obs) – I (cal), is shown in the lower part of the figure. The inset is an enlarged view of the (202) and (040) peak.

Detailed X-ray powder diffraction was performed on the sample $Bi_{0.5}Sr_{0.5}MnO_3$ from 570 K to 300 K. The evolutions of the lattice parameters of the MA phase and MI phase were determined from the refinements of the XRD patterns and shown in Fig. 6. The lattice parameter b of both the phases decreased on cooling and shrunk saliently around the phase separation temperature, accompanied by an increase in a and c. This is the feature of cooperative Jahn–Teller distortions of the MnO_6 octahedrons and may indicate an ordering of the occupied $d_{3x^2-r^2}$ and $d_{3z^2-r^2}$ orbitals on the ac plane. The inset shows the temperature dependence of the phase fraction from 300 K to 500 K for the MI phase. The phase fraction decreases slightly up to 400 K, rapidly above 400 K and approaches zero at approximately 480 K, around which the magnetization, resistivity, and thermoelectric power exhibit anomalies. Figure 6 shows that the lattice parameter b is almost equal for the MA and MI phases, while the lattice parameters a and c of the MA phase exhibit an obvious and continuous change around the phase separation temperature. Extrapolating the lattice parameters to high temperatures, it seems that the a and c of the MI phase exhibit much smaller changes around the phase separation temperature than those of the MA phase. These features may imply different orbit-ordering modes or difference in degree of orbit-ordering on the ac plane between the MA and MI phases, since the decrease of the b axis and the increases of a and c axes essentially originate from the cooperative Jahn–Teller distortion of $Mn^{3+}O_6$ octahedrons and an ordering of the e_g orbitals on the ac plane. Based on the above observations, we can attribute the anomalies in magnetization, resistivity, and thermoelectric power of $Bi_{1-x}Sr_xMnO_3$ to the phase separation rather than to the charge-ordering transition.

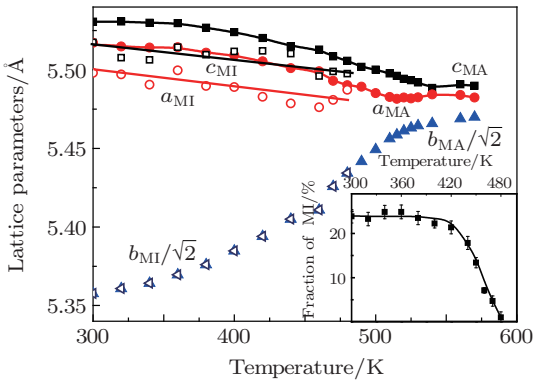


Fig. 6. (color online) Temperature dependence of the refined lattice parameters for the two phases. The opened circle, square, and triangle denote the parameters a_{MI}, b_{MI}, and c_{MI} of the MI phase. The solid circle, square, and triangle denote the parameters a_{MA}, b_{MA}, and c_{MA} of the MA phase. The inset shows the temperature dependence of the phase fraction of MI phase.

In order to check if the CO state exists in our investigated polycrystalline $Bi_{1-x}Sr_xMnO_3$, a series of experiments were conducted. The high resolution XRD and NPD data (below the reported T_{CO}) shows no trace of the superstructure reflections corresponding to the Mn^{3+}/Mn^{4+} charge ordering. The electron diffraction was also performed and the pattern shows no superlattice spots besides the fundamental Bragg reflections. Though some imaging conditions such as specimen thickness, orientation, electron beam intensity, and microscopy aberrations may influence the electron diffraction patterns, a global long-range charge-order state does not seem to exist in our investigated $Bi_{1-x}Sr_xMnO_3$ samples. It has been speculated that the charge ordering may occur locally in $Bi_{1-x}Ca_xMnO_3$ compounds, but the coherence length of the ordered domains may be too small to be detected by diffraction techniques.[9,14]

4. Conclusion

In summary, studies on the evolution of the crystal structure of the polycrystalline $Bi_{1-x}Sr_xMnO_3$ ($x = 0.4$–0.6) by temperature-dependent high resolution X-ray powder diffraction and high resolution neutron powder diffraction show that these polycrystalline samples manifest a phase separation at the temperature close to the reported T_{CO} for the compounds. Anomalies in magnetization, resistivity, and thermoelectric power are observed around the phase separation temperature. Both the separated phases crystallize in the orthorhombically distorted perovskite structure with space group *Imma*. At low temperature, the majority (MA) phase orders in the A-type AFM structure and the minority (MI) phase orders in the CE-type AFM structure. However, the detailed XRD and NPD

data and electronic diffractions show no evidence of long-range charge-ordering in all three investigated samples below the reported T_{CO}. Therefore, the reported high T_{CO} of the Bi-based perovskite manganites derived from anomalies in the physical properties should be reconsidered.

References

[1] Tokura Y and Nagaosa N 2000 *Science* **288** 462
[2] Dagotto E, Hotta T and Moreo A 2001 *Phys. Rep.* **344** 1
[3] Goodenough J B 1955 *Phys. Rev.* **100** 564
[4] Moreo A, Yunoki S and Dagotto E 1999 *Science* **283** 2034
[5] Woo H, Tyson T A, Croft M, Cheong S W and Woicik J C 2001 *Phys. Rev. B* **63** 134412
[6] García-Muñoz J L, Frontera C, Aranda M A G, Llobet A and Ritter C 2001 *Phys. Rev. B* **63** 064415
[7] Frontera C, García-Muñoz J L, Ritter C, Mañosa L, Capdevila X G and Calleja A 2003 *Solid State Commun.* **125** 277
[8] Hervieu M, Maignan A, Martin C, Nguyen N and Raveau B 2001 *Chem. Mater.* **13** 1356
[9] Giot M, Beran P, Pérez O, Malo S, Hervieu M, Raveau B, Nevriva M, Knizek K and Roussel P 2006 *Chem. Mater.* **18** 3225
[10] Radaelli P G, Cox D E, Capogna L, Cheong S W and Marezio M 1999 *Phys. Rev. B* **59** 14440
[11] Kuwahara H, Tomioka Y, Asamitsu A, Moritomo Y and Tokura Y 1995 *Science* **270** 961
[12] Bao W, Axe J D, Chen C H and Cheong S W 1997 *Phys. Rev. Lett.* **78** 543
[13] Martin C, Maignan A, Hervieu M, Raveau B, Jirák Z, Kurbakov A, Trounov V, André G and Bourée F 1999 *J. Magn. Magn. Mater.* **205** 184
[14] Santhosh P N, Goldberger J, Woodward P M, Vogt T, Lee W P and Epstein A J 2000 *Phys. Rev. B* **62** 14928
[15] Frontera C, García-Muñoz J L, Aranda M A G, Ritter C, Llobet A, Respaud M and Vanacken J 2001 *Phys. Rev. B* **64** 054401
[16] Wollan E O and Koehler W C 1955 *Phys. Rev.* **100** 545
[17] Kim B H, Kim J S, Kim M S, Zhang C J, Kim K H, Kim B G, Kim H C and Park Y W 2006 *Phys. Lett. A* **351** 368
[18] Mantytskaya O S, Troyanchuk I O, Chobot A N and Szymczak H 2004 *Low Temp. Phys.* **30** 218
[19] Frontera C, García-Muñoz J L, Llobet A, Aranda M A G, Ritter C, Respaud M and Vanacken J 2001 *J. Phys.: Condens. Matter* **13** 1071